

Geometric coupling impedance of LHC secondary collimators

**Oscar Frasciello¹, S. Tomassini¹, M. Zobov¹,
A. Grudiev², E. Metral², N. Mounet², B. Salvant²**

¹INFN, Laboratori Nazionali di Frascati, Rome, Italy

²CERN, Geneva, Switzerland

TWIICE 2014, Topical Workshop on Instabilities, Impedances
and Collective Effects

Synchrotron SOLEIL, January 16th, 2014



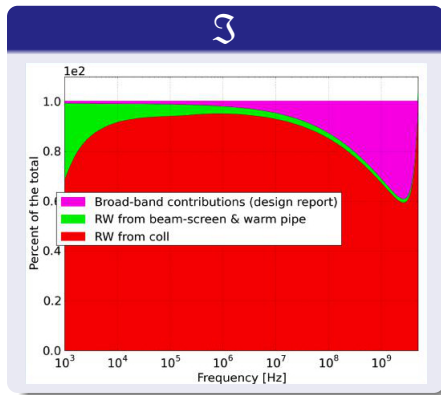
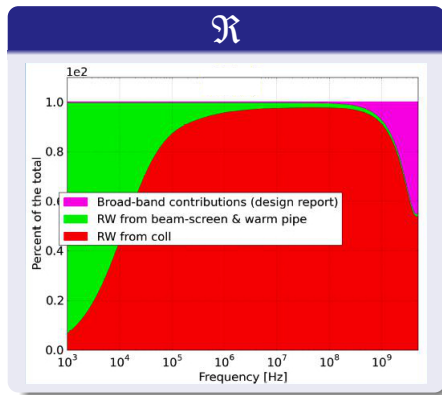
The HLumi LHC Design Study is included in the High Luminosity LHC project and is partly funded by the European Commission within the Framework Programme 7 Capacities Specific Programme. Grant Agreement 284404



Laboratori Nazionali di Frascati

- Importance of the collimators impedance
- Geometric impedance: theoretical considerations
- Geometric impedance: simulation results
- The LHC impedance model update
- Conclusions and future plans

Details of collimators contribution in %



(Courtesy of N. Mounet)

The goal

Increase the LHC luminosity by an order of magnitude

The goal

Increase the LHC luminosity by an order of magnitude

How to

One of the key tasks is to increase the beam intensity

The goal

Increase the LHC luminosity by an order of magnitude

How to

One of the key tasks is to increase the beam intensity

Something to keep under control...

- Beam instabilities;
- Excessive power losses;

The goal

Increase the LHC luminosity by an order of magnitude

How to

One of the key tasks is to increase the beam intensity

Something to keep under control...

- Beam instabilities;
- Excessive power losses;

...what can be done

- Careful design of new vacuum chambers;
- Present LHC impedance model improvement;

The goal

Increase the LHC luminosity by an order of magnitude

How to

One of the key tasks is to increase the beam intensity

Something to keep under control...

- Beam instabilities;
- Excessive power losses;

...what can be done

- Careful design of new vacuum chambers;
- Present LHC impedance model improvement;

LHC collimators are among the main beam coupling impedance contributors.

Simulations vs. measurements

- The measured tune shifts are higher than predicted ones by around a factor of 2;
- The existing LHC impedance model accounts only for a fraction, $\sim \frac{1}{3} - \frac{1}{2}$, of the measured transverse coherent tune shifts;

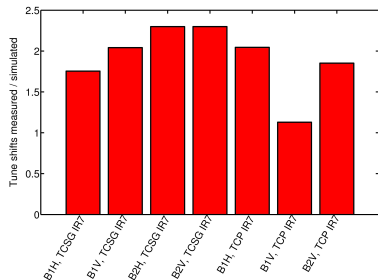


Needs for LHC impedance model refining.

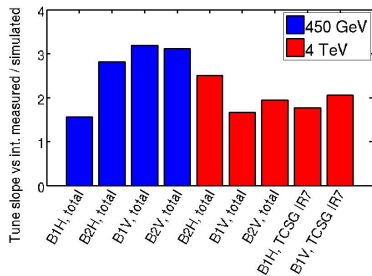
Tune shifts simulations vs. measurements

Tune shifts measurements were performed comparing tune slope wrt intensity between simulations and measurements; $Q' \sim 1 - 5$

Collimator tune shifts



Total tune shifts



(Courtesy of N. Mounet)

Geometric Impedance: theoretical considerations I

- Since Bane and Morton work [1], it's possible to identify two different physical mechanisms for wake generation:
 - ① $\rho = 0$ (perfectly conducting wall), electric and magnetic forces acting on the beam from the image charges do not cancel completely \Rightarrow **Geometric wake**;
 - ② $\rho \neq 0$ (finite wall conductivity) \Rightarrow **Resistive wake**;
- Resistive Wall (RW) impedance considered as the dominant contribution for LHC collimators impedance;
- In the “old” LHC model, geometric impedance was accounted only in terms of round taper approximation.

Let's try to understand the factor of 2 arising from LHC collimators comparing the kick factors due to resistive wall impedance and the geometric impedance:

- 1 It's a quite straightforward way ;
- 2 Contributions from impedances having different frequency behaviour into the transverse tune shifts can be easily compared;
- 3 Only calculations of the broad band wakes are necessary without the exact knowledge of $Z(\omega)$;
- 4 Easily calculated by many numerical codes.

Given $\xi = 0$ and ($m = 0$) in Sacherer's formula [2] for coherent mode frequency shift, one gets:

$$\Delta\omega_{c_0} = -C \cdot I \sum_p \Im Z_T(\omega_p) e^{-\left(\frac{\omega\sigma_z}{c}\right)^2} \quad (1)$$

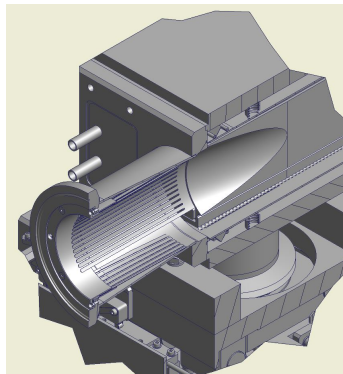
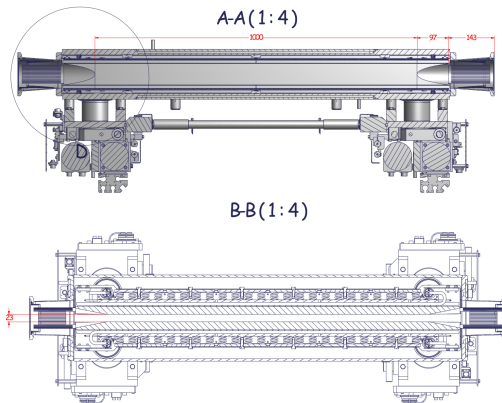
But from kick factor definition:

$$k_T = \frac{1}{2\pi} \int_{-\infty}^{\infty} \Im Z_T(\omega) |\lambda(\omega)|^2 d\omega = \frac{1}{2\pi} \int_{-\infty}^{\infty} \Im Z_T(\omega) e^{-\left(\frac{\omega\sigma_z}{c}\right)^2} d\omega \quad (2)$$

so that:

$$\boxed{\Delta\omega_0 \propto -k_T} \quad (3)$$

LHC secondary collimator CAD design



(Courtesy of CERN collimation team, EN/MME and Luca Gentilini)

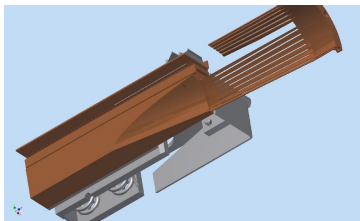
What an “old” wise man can teach...

- 1 For structures with long tapers, longitudinal and transverse wake potentials show unphysical behaviour;
- 2 The reasons for this numerical behaviour still remain unknown;
- 3 An overcome can be:

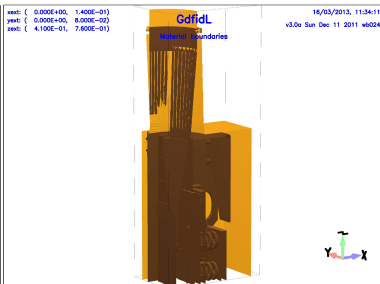
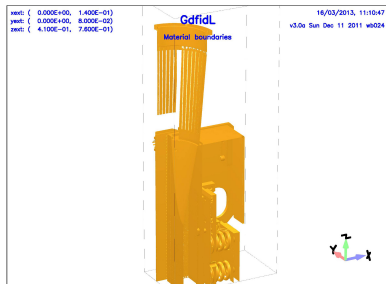
$$\boxed{\frac{a\phi}{\Delta z} \cdot \frac{\sigma_z}{\Delta z} \geq 100} \quad (4)$$

...an “accuracy criterion” from ABCI manual.

GdfidL electromagnetic code model



Very fine mesh needed for taper structure. We used 0.2 mm in all three directions, leading to several billions of mesh points \Rightarrow very huge computing task!

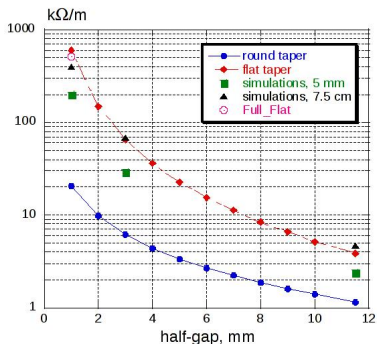


For a smooth taper, for example, it can be shown [3] that:

$$k_T = \int_0^{\infty} G\left(\frac{\omega}{c} \sigma_z\right) \Re Z_T(\omega) d\omega - \frac{c}{2\pi^{1/2} \sigma_z} \Im Z_T(0) \quad (5)$$

- If $\Re Z_T(\omega) \ll \Im Z_T(\omega)$, $k_T \propto \Im Z_T(0)$;
- Calculation of $\Im Z_T(0)$ is much easier to perform than $Z_T(\omega)$, because it involves only solutions of Maxwell equations for static fields.

Low frequency broad-band transverse impedance

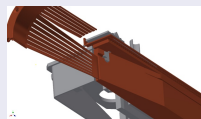


Models

$$① \quad Z_T = j \frac{Z_0}{2\pi} \int \left(\frac{b'}{b} \right)^2 dz;$$

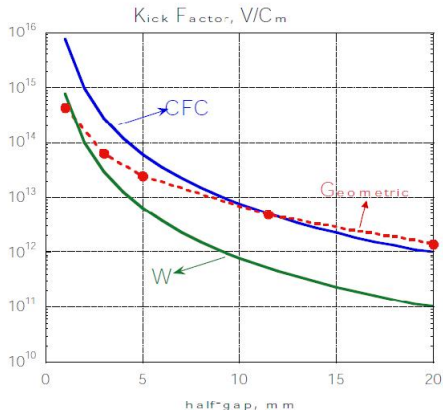
$$② \quad Z_T = j \frac{Z_0 w}{4} \int \frac{(g')^2}{g^3} dz;$$

The Stupakov [4] model in item 2 is closer to simulated points than that of Yokoya [5] in item 1; there's only one point for the “full-flat” geometry below:



Geometric impedance: simulations II (\perp)

kick factor comparison

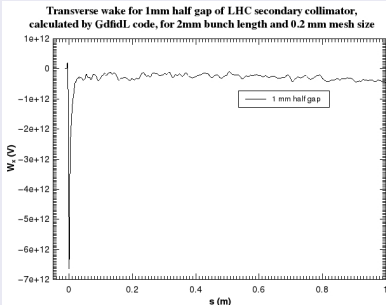


kick factor analysis results

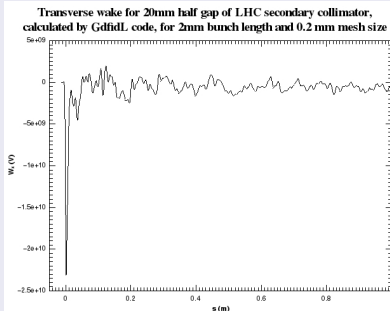
- For W collimators, geometrical impedance contribution dominates in the whole range of half gaps, while only from ≈ 8 mm onward it does for CFC collimators;
- Even considering the partial contribution in the case of CFC, it is evident that the geometrical impedance is absolutely not negligible wrt RW one.

Geometric impedance: simulations II (\perp)

1 mm half gap geometry

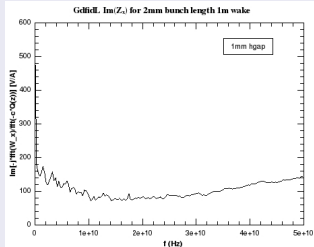
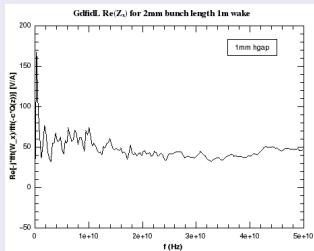


20 mm half gap geometry

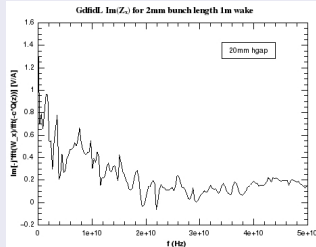
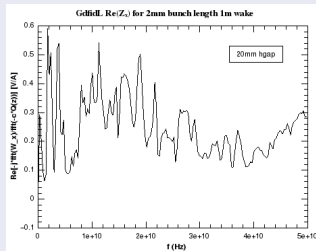


Geometric impedance: simulations II (\perp)

1 mm half gap geometry

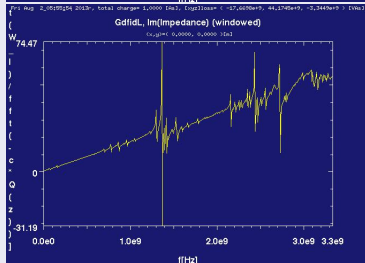
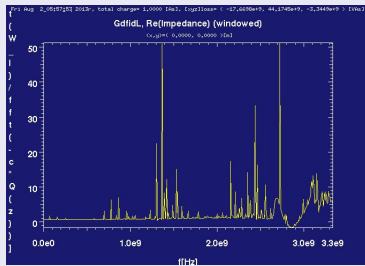


20 mm half gap geometry

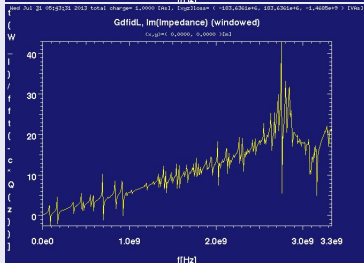
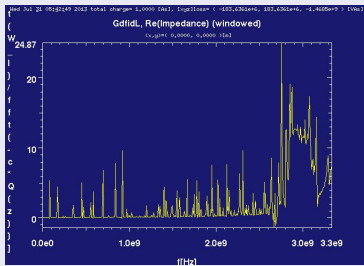


Geometric impedance: simulations II (||)

1 mm half gap geometry



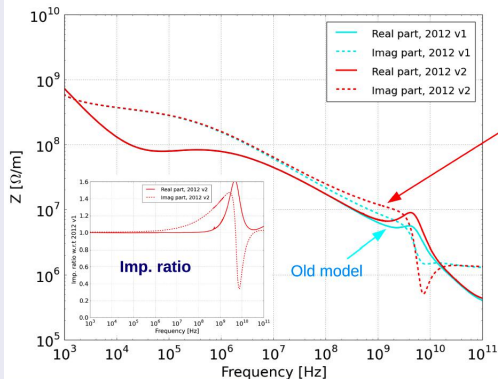
20 mm half gap geometry



The longitudinal impedance exhibits many resonant peaks at different frequencies. As also shown in the earlier work of A.Grudiev [6], these HOMs are the modes created in the collimator tank, trapped between sliding contacts in the tapered transition area etc. with parameters depending very much on the collimator gap size. Despite their shunt impedances are relatively small compared to typical HOMs in RF cavities, possible further RF losses and related collimator heating, due to these modes, in the conditions of higher circulating currents still need a deeper investigation.

The LHC impedance model

Vertical dipolar impedance for LHC 2012 (4 TeV) physics settings



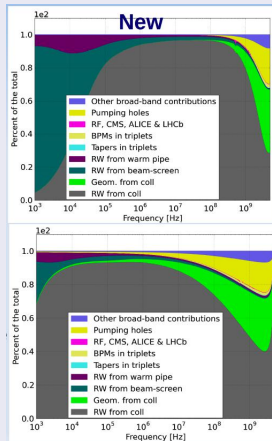
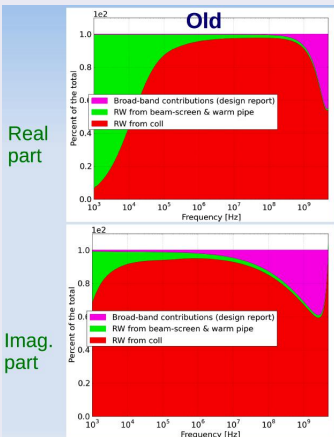
New model

→ Low frequency impedance stays the same,
→ visible increase at high frequency.

(Courtesy N. Mounet)

The LHC impedance model

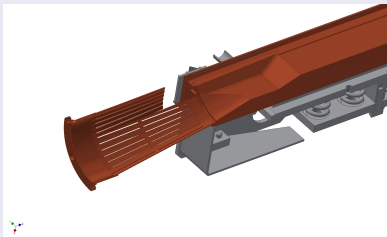
Details of the various contributions in %



(Courtesy of N. Mounet)

Not only one collimator design...

Collimator taper with BPM cavity



LHC collimators with and without BPM cavity impedance comparison

	With BPM cavity	Without BPM cavity
Half gaps (mm)	$k_l \left(\frac{V}{Cm} \right)$	$k_l \left(\frac{V}{Cm} \right)$
1	$3.921 \cdot 10^{14}$	$3.340 \cdot 10^{14}$
3	$6.271 \cdot 10^{13}$	$5.322 \cdot 10^{13}$
5	$2.457 \cdot 10^{13}$	$2.124 \cdot 10^{13}$

The transverse effective impedance is expected to increase of about 20% wrt no BPM cavity collimator design.

Conclusions and future plans I

- Calculations of wake fields and beam coupling impedance have been performed for the LHC secondary collimators, for five different gaps, by means of GdfidL electromagnetic code;
- From the comparison of the transverse kick factors, it has been shown that the geometric impedance contributions is not negligible with respect to the resistive wall one;
- In particular, for CFC made collimator, the geometrical kick starts to be comparable to RW one at about 8 *mm* half gap. In turn, for W made collimators, the geometrical kick dominates almost for all the collimator gaps;

Conclusions and future plans II

- The present study has contributed to the refinement of the LHC impedance model. It has also been shown that the geometrical collimator impedance accounts for approximately 30% of the total LHC impedance budget, at frequencies close to 1 GHz ;
- The work is still in progress in order to understand the origin and strenghts of the HOMs trapped in the complicated collimator structure;
- Beam impedance simulations for the new collimators, modified for the HiLumi-LHC upgrade, has just been started.

- [1] K. L. F. Bane and P. L. Morton.
Deflection by the image current and charges of a beam scraper.
Proceedings of the 1986 Linac Accelerator Conference, page 490,
1986.
- [2] B. Zotter and F. Sacherer.
Transverse instabilities of relativistic particle beams in
accelerators and storage rings.
Conf.Proc., C761110:175–218, 1976.
- [3] G.V. Stupakov.
Geometrical wake of a smooth taper.
Part.Accel., 56:83–97, 1996.

- [4] G. Stupakov.
Low Frequency Impedance of Tapered Transitions with Arbitrary Cross Sections.
Phys.Rev.ST Accel.Beams, 10:094401, 2007.
- [5] Kaoru Yokoya.
Resistive wall impedance of beam pipes of general cross-section.
Part.Accel., 41:221–248, 1993.
- [6] A. Grudiev.
Simulation of longitudinal and transverse impedances of trapped modes in lhc secondary collimator.
CERN AB-Note-2005-042, 2005.
- [7] Robert L. Gluckstern, Johannes van Zeijts, and Bruno Zotter.
Coupling impedance of beam pipes of general cross-section.
Phys.Rev., E47:656–663, 1993.

Thanks for your kind attention

Sacherer's formula [2] for coherent mode frequency shift:

$$\Delta\omega_{c_m} = j \frac{1}{1 + |m|} \frac{I_c^2}{4\pi f_0 Q(E/e)L} Z_m^{eff} \quad (6)$$

m azimuthal mode number; f_0 revolution frequency; I average bunch current; Q betatron tune; E machine energy; L full bunch length. The Z_m^{eff} is calculated over a coherent mode power spectrum:

$$Z_m^{eff} = \frac{\sum_p Z_T(\omega_p) h_m(\omega_p - \omega_\xi)}{\sum_p h_m \omega_p - \omega_\xi} \quad (7)$$

For a given mode m , the bunch power spectrum is given by:

$$h_m(\omega) = \left(\frac{\omega \sigma_z}{c} \right)^{2|m|} e^{-\left(\frac{\omega \sigma_z}{c} \right)^2} \quad (8)$$

The sum in 7 is performed over the mode spectrum lines:

$$\boxed{\omega_p = (p + \Delta Q) \omega_0 + m \omega_s \quad ; \quad -\infty < p < +\infty} \quad (9)$$

The “chromatic” angular frequency is given by

$$\omega_\xi = \omega_0 \frac{\xi}{\eta}$$

Given purely imaginary tune shifts from equation 6, they assume real values for imaginary transverse impedance. For $\xi = 0$ and coherent mode ($m = 0$) we get a proportionality relation:

$$\Delta\omega_{c_0} = -C \cdot I \sum_p \Im Z_T(\omega_p) e^{-\left(\frac{\omega\sigma_z}{c}\right)^2} \quad (10)$$

But from kick factor definition:

$$k_T = \frac{1}{2\pi} \int_{-\infty}^{\infty} \Im Z_T(\omega) |\lambda(\omega)|^2 d\omega = \frac{1}{2\pi} \int_{-\infty}^{\infty} \Im Z_T(\omega) e^{-\left(\frac{\omega\sigma_z}{c}\right)^2} d\omega \quad (11)$$

so that, comparing with 10, we find

$$\boxed{\Delta\omega_0 \propto -k_T} \quad (12)$$

Equation 11, under specified conditions, has general validity. In order to evaluate RW kicks, we can consider the thick wall impedance of a flat vacuum chamber [7] with $2a \cdot 2b$ cross section:

$$\frac{Z_{T_y}}{L} = \frac{(1+j)Z_0\delta}{2\pi b^3} F_{1y} \left(\frac{b}{a} \right) \quad (13)$$

with $\delta = \sqrt{\frac{2c\rho}{\omega Z_0}}$ skin depth and $Z_0 = 120 \pi \Omega$ free space impedance.

$$\begin{aligned} Z_{T_y} &= \frac{L(1+j)Z_0\delta}{2\pi b^3} F_{1y} \left(\frac{b}{a} \right) = \frac{LZ_0\delta}{2\pi b^3} F_{1y} \left(\frac{b}{a} \right) + j \frac{LZ_0\delta}{2\pi b^3} F_{1y} \left(\frac{b}{a} \right) \\ \Im Z_T &= \Im Z_{T_y} = \frac{LZ_0\delta}{2\pi b^3} F_{1y} \left(\frac{b}{a} \right) \end{aligned} \quad (14)$$

Appendix: Theoretical considerations II exploited

Substituting 14 into 11 we get after some simple algebra:

$$k_T = \frac{L}{2\pi^2 b^3} \sqrt{2c\rho Z_0} F_{1y} \left(\frac{b}{a}\right) \int_0^\infty \frac{1}{\sqrt{\omega}} e^{-\frac{\omega^2 \sigma_z^2}{c^2}} d\omega;$$

$\int_0^\infty \frac{1}{\sqrt{\omega}} e^{-\frac{\omega^2 \sigma_z^2}{c^2}} d\omega$ is an Euler Γ function

$$\Gamma(z) = \int_0^\infty e^{-t} t^{z-1} dt,$$

with $z = 0$. So that:

$$\int_0^\infty \frac{1}{\sqrt{\omega}} e^{-\frac{\omega^2 \sigma_z^2}{c^2}} d\omega = 2\Gamma\left(\frac{5}{4}\right) \frac{1}{\sqrt{\frac{\sigma_z}{c}}}$$

and we've

$$k_T = \frac{L}{2\pi^2 b^3} \sqrt{2c\rho Z_0} F_{1y} \left(\frac{b}{a}\right) 2\sqrt{\frac{c}{\sigma_z}} \Gamma\left(\frac{5}{4}\right) \quad (15)$$

For a flat rectangular vacuum chamber, the form factor

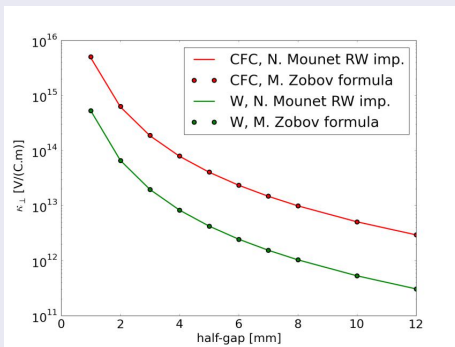
$$F_{1y} \left(\frac{b}{a} \right) = \frac{\pi^2}{12}$$

so that, finally, the RW contributions:

$$k_T = \frac{Lc}{12b^3} \sqrt{\frac{2Z_0\rho}{\sigma_z}} \Gamma \left(\frac{5}{4} \right) \quad (16)$$

Just as remark, note that the same type of calculations hold for $Z_T^x(\omega)$ but taking into account that $F_{1x} \left(\frac{b}{a} \right) = \frac{\pi^2}{24}$, so leading to a weaker vertical kick.

Comparison between LHC impedance model (RW) and equation 16



(Courtesy N. Mounet)